Energy Conversion and Management 78 (2014) 405–411

Contents lists available at ScienceDirect

Energy Conversion and Management

journal homepage: www.elsevier.com/locate/enconman

Exergy analysis and optimization of Dieng single-flash geothermal power plant

Nugroho Agung Pambudi [a,*], Ryuichi Itoi [a], Saeid Jalilinasrabady [a], Khasani Jaelani [b]

[a] Energy Resources Engineering Laboratory, Faculty of Engineering, Kyushu University, 744 Motooka, Nishi-ku, Fukuoka 819-0395, Japan
[b] Department of Mechanical and Industrial Engineering, Faculty of Engineering, Gadjah Mada University, Yogyakarta 55281, Indonesia

ARTICLE INFO

Article history:
Received 17 July 2013
Accepted 30 October 2013
Available online 26 November 2013

Keywords:
Dieng geothermal field
Optimization
Single-flash
Exergy analysis
Geothermal power plant

ABSTRACT

Exergy analysis and optimization of a single-flash geothermal power plant are conducted by developing a mathematical model that is applied to the Dieng geothermal power plant in Indonesia. Calculations are conducted by using the Engineering Equation Solver (EES) code using methods based on the laws of thermodynamics. The exergy flow and efficiency are computed at several plant components, including the separator, turbine, condenser, and for the whole power plant.

The exergy of the geothermal fluid that is discharged from the production wells is estimated to be 59.52 MW. This amount of fluid produces 21.71 MW of electricity from the power plant overall, with second law efficiency to be 36.48%. There is a considerable amount of waste brine, amounting to 17.98% (10.70 MW) of the total available exergy, which is disposed of in the plant's reservoir. The optimization of the plant is carried out by adjusting the separator pressure. The results show that a slight increase of 20 kW in the output power can be attained by lowering the separator pressure to 9 bar from 10 bar. The Grassmann diagram shows the exergy losses at each component in the power plant. The turbine and separator losses are 7.51 MW (12.62%) and 8.04 MW (13.5%), respectively, while the cooling tower has an exergy loss of 2.62 MW (4.40%). The total condenser loss is 5.8 MW (9.75%).

1. Introduction

Geothermal energy has been identified as an energy resource that is both sustainable and a low emission producer [1]. Ármannsson et al. [2] reported that this resource has low CO_2 emission characteristics. Geothermal energy is also the non-intermittent resources to provide base-load electricity [3]. The use of geothermal energy for electricity generation was initially realized in Lardrello, Italy in 1904, where geothermal steam was used to drive a small turbine that was used to power light bulbs. This program was prolonged and in 1913, a plant with a 250 kW capacity was connected to the Italian grid system [4]. The development of geothermal power plants has continued up to the present day, using various technologies including dry steam, and flash and binary cycles. Bertani [5] reported that geothermal power plants worldwide produced 10,898 MW of power and generated 67,246 GW h of electricity as of 2010. Despite the small amount of electricity produced by geothermal generation, the future development of this technology is becoming attractive because of increasing fossil-fuel costs as the sources of these fuels are becoming depleted [6].

With the great potential for use of geothermal energy, Indonesia is planning to increase its geothermal electricity production from 1196 to 9500 MW by 2025. To achieve that target, an appropriate policy is required to encourage the geothermal industry. At present, the total installed geothermal power plant capacity in Indonesia is 1196 MW from seven power plant locations: Darajat (260 MW), Dieng (60 MW), Kamojang (200 MW), Gunung Salak (377 MW), Sibayak (12 MW), Lahendong (60 MW), and Wayang Windu (227 MW) [7].

The developments of geothermal power plants have two ways: the construction of new power plants with new fields and improvements in the thermal efficiency of the existing power plant. These thermal efficiency improvements can be realized by the use of exergy and energy analyses. These analyses have been used by several researchers as powerful tools to identify and quantify energy-degrading processes, because it enables the types, locations and quantities of the energy losses to be evaluated [8].

A thermodynamic evaluation was conducted in the Kizildere geothermal power plant in Denizli, Turkey by [9]. Ozgner et al. [10] conducted a comprehensive energy and exergy analysis of the Salihli geothermal district heating system and its essential components. Balli et al. [11] produced an exergetic performance assessment of a combined heat and power system installed in Eskisehir, Turkey in their study. In the study performed by Rosen et al. [12], the increase in the exergy storage capacity that was attained

* Corresponding author.
E-mail address: Pambudi@kyudai.jp (N.A. Pambudi).

0196-8904/$ - see front matter © 2013 Elsevier Ltd. All rights reserved.
http://dx.doi.org/10.1016/j.enconman.2013.10.073

Nomenclature

h_i	specific enthalpy at stream i (kJ/kg)	$\dot{W}$	power output (MW)
h_0	specific enthalpy at environmental state (kJ/kg)	$\dot{X}_{out}$	desired exergy output (kW)
$\dot{m}_i$	mass flow rate at stream I (kg/s)	$\dot{X}_{in}$	necessary exergy input (kW)
ppm	parts per million	$\dot{X}_i$	exergy (kW)
s_i	specific entropy at stream i (kJ/kg K)	η_t	isentropic efficiency
s_0	specific entropy at environmental state (kJ/kg K)	η_{II}	second law efficiency
T_0	temperature at environmental state (K)		
W	work (MW)		

in thermal storage facilities through stratification was assessed by using a design-oriented temperature-distribution model for vertically stratified thermal storage. It is important to use a holistic approach in the design of energy devices or processes to ensure maximum safety, minimize the use of limited energy resources, use renewable resources, minimize waste of all kinds, and develop new technologies to improve energy efficiency [13]. A comparison of the main approaches to second-law analysis was reported in the literature in [14].

The present research aims to analyze the performance of the single-flash geothermal power plant in Dieng by applying exergy and energy analysis using the laws of thermodynamics. The results of the analysis are used to optimize the separator pressure to enhance the efficiency of the power plant and thus achieve higher output power. The Engineering Equation Solver (EES) code is used to simulate the single-flash system based on a plant model that uses actual and designed data.

2. Dieng geothermal field and power plant

The Dieng plateau is located at an elevation of 2000 m above sea level in the southern central region of the Java province in Indonesia, and has an annual average ambient temperature of 18 °C [15]. The atmospheric pressure in Dieng is 78.06 kPa, according to the local meteorological agency [16]. This plateau is a volcanic path, where the surface manifestations of geothermal activities such as hot springs and fumaroles are present. There are also craters, such as Sileri in the north and Sikidang and Pakuwaja in the south. Dieng was identified as one of the most significant geothermal prospects in Indonesia. Between 1970 and 1972, the Sikidang sector of the Dieng volcanic complex was investigated under the auspices of a United States Agency for International Development (USAID) program [17]. Prasetio et al. [18] reported that the Dieng reservoir is characterized by the presence of a steam–water two-phase condition in a liquid-dominated reservoir within a temperature range from 240 °C to 333 °C.

The Dieng geothermal power plant has adopted a single-flash system with an installed capacity of 60 MW and is supplied by steam from eight production wells at four locations. There are five production wells active, in wellpads 1, 3, and 4, as of November 2011. Productions wells 2A and 2B were in an offline condition at that time.

Fig. 1 shows the steam and brine gathering system at the plant, including the two-phase lines from the wells. When the plant data were collected, the system used four satellite separators to deliver the steam to the power plant. These satellite separators are located within the wellpads, which are located far away from the power house, such as wellpad 1, which is located approximately 4.6 km from the power house, and wellpad 3, which is located approximately 2 km from the power house. This gathering system is required to collect the steam from several separators that are flowing to the power house and to collect the brine that is flowing to the reinjection well. Wellpad 1 has three separators and wellpads 2 and 3 have two separators. Wellpad 4 has one separator that is used only for Well-4. Wellpad 1 has three production wells: Well-1A, Well-1B, and Well-1C; wellpad 2 has two production wells: Well-2A and Well-2B; and wellpad 3 has two production wells: Well-3A and Well-3B.

There are two reinjection wells: INJ-1, located in the northern part of the field, and INJ-2, which is in the southern part of the field. The separated brine from wellpads 1 and 2 is sent to well INJ-1, while the brine from wellpads 3 and 4 is sent to well INJ-2. The Dieng power plant uses a cold brine injection system that injects brine under relatively low temperature conditions. This system has been used to avoid scaling problems in the reinjection process because of the high silica concentration in brine, which is more than 1000 ppm. The brines are sampled at each wellpad and their silica concentrations are analyzed by the molybdenum yellow method in the laboratory. The separated brine is sent to the flasher located in the wellpad, and the brine is also sampled at the outlet of the flasher. The analysis results are summarized in Table 1. The total silica concentrations of the brines from wellpads 1 and 3 are 1442 and 1145 ppm, respectively.

The brine is discharged from the flasher then flows through the canal to the pond. A hot reinjection system was used at one time, but the high silica content of the brine frequently caused pump damage and led to the adoption of the present system for brine treatment.

Fig. 2 presents a schematic diagram of an existing single-flash power plant producing 21.71 MW of electricity based on the data obtained from the plant in November 2011. The geothermal fluid is produced from the reservoir through the well and is separated into steam and brine in the separator. The power plant is modeled into a simplified design assuming a single production well in one separator. The separator pressure in the plant is equal to 10 bar which is an average pressure at satellite separators.

In the separation process in the separator, steam and liquid is separated at a specific pressure. Enthalpy of two-phase fluid enters the separator and its enthalpy is determined by assuming single-phase liquid water in the reservoir at specific temperature. The dryness fraction in the separator is calculated with following equation:

$$X_2 = \frac{h_1 - h_3}{h_2 - h_3} \tag{1}$$

where X_2 is the dryness fractions, h_1 is the fluid enthalpy at the separator inlet, h_2 is the enthalpy of steam at the separator exit, h_3 is the enthalpy of brine. Enthalpy of steam is determined by properties of the separator pressure under saturated vapor condition.

The separated steam from the separators, indicated by number 2, flows into the power house while the brine, indicated by number 22, goes first to the flasher, then flows into the canal, and finally flows to the pond before being pumped to the reinjection wells.

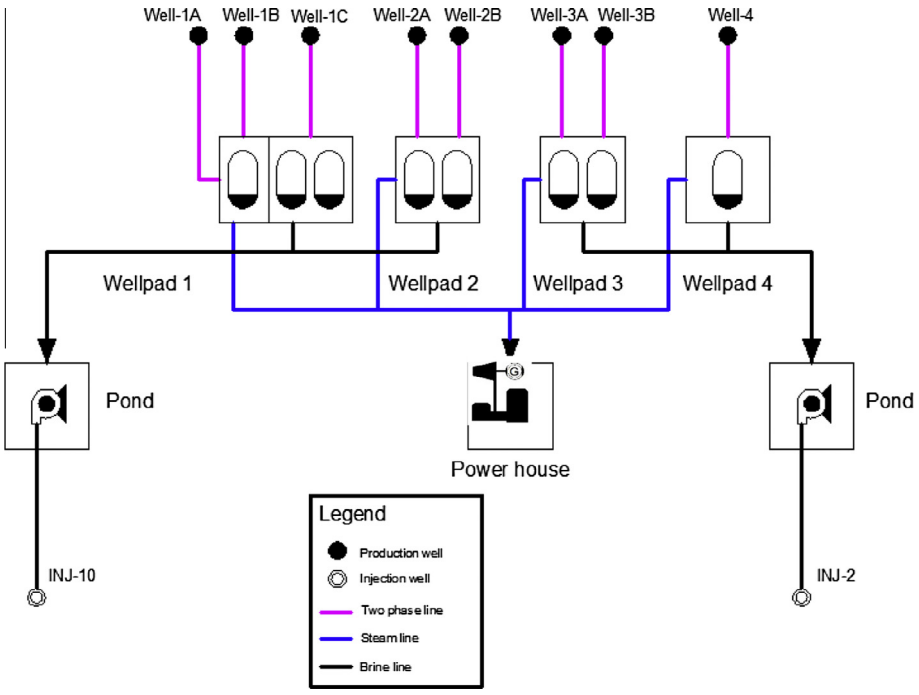

Fig. 1. Steam and brine gathering system and satellite separators.

Table 1
Important parameters for the major stages of a single-flash power plant.

State	Enthalpy (kJ/kg)	Pressure P (bar)	Entropy s (kJ/kg K)	Mass flow (kg/s)	Energy (kW)	Temperature (°C)	Exergy (kW)
0	75.54	0.78	0.2676			18	
1	1401	10	3.349	138.9	194,631	179.9	59,518
2	2778	10	6.586	44.01	122,240	179.9	37,959
3	2777	9.79	6.593	43.99	122,155	178.6	37,815
4	758.8	9.79	2.13	0.01762	13.37	179.9	2.486
5	2777	9.79	6.593	40.78	113,237	172.5	35,054
6	2245	0.07	7.226	40.78	91,527	38	5832
7	134		0.464	4354	300,899	34.3	2898
8	92.33	1.42	0.3949	4098	189,196	27	364.6
9	1432		4.647	1.014	1452	38	88.01
10	2777	9.79	6.593	1.356	3767	172.5	1166
11	2777	9.79	6.593	1.855	5152	172.5	1595
12	2202		5.761	2.37	5218		1254
13	167.5		0.5723	89.34	10,856	40	210
14	92.41	2.1	0.3949	88.31	5894	27	99.15
15	1710	1.076	5.465	1.333	2280		167
16	2331		6.121	3.188	7431		1762
17	167.5		0.5723	129.1	15,741	40	304.5
18	135.5	2.26	0.4681	126.3	12,362	27	143.3
19	1473	0.78	4.747	0.4486	660.8	40	102.8
20	75.54	0.78	5.841	1.963	148.2	18	0
21	117.6	0.78	0.4095	0.04163	4.895		67.58
22	762.9	10	2.139	94.89	72,392	179.9	13,523
23	2664	0.78	7.442	15.6	41,550	92.85	7795
24	388.9	0.78	1.225	79.3	30,841	92.85	2736

Some scaling problems have been found in the pipeline because of the silica concentration in the brine.

When the steam arrives at the power house, it is then purified with a scrubber to increase the quality of the steam and to avoid allowing any fouling material that is trapped on the steam into the power house. The steam indicated by number 3 then flows into the turbine and generates electricity. The data of mass flow rate, temperature and pressure of the inlet of this turbine is provided on the data plant. The steam from the turbine exhaust, indicated by number 6, then flows to the condenser at a pressure 0.07 bar and a temperature 38 °C.

In the turbine, work output is calculated using Eq. (2).

$$\dot{W}_t = \dot{m}_5(h_5 - h_6)\eta_t \tag{2}$$

where $\dot{W}_t$ is the work output, h_5 is enthalpy of the turbine inlet, h_6 is enthalpy of the turbine outlet. Since the enthalpy of turbine outlet, h_6, is unknown isentropic condition at Eq. (3) applies for calculating that h_6.

$$\eta_t = \frac{(h_5 - h_6)}{h_5 - h_{6s}} \tag{3}$$

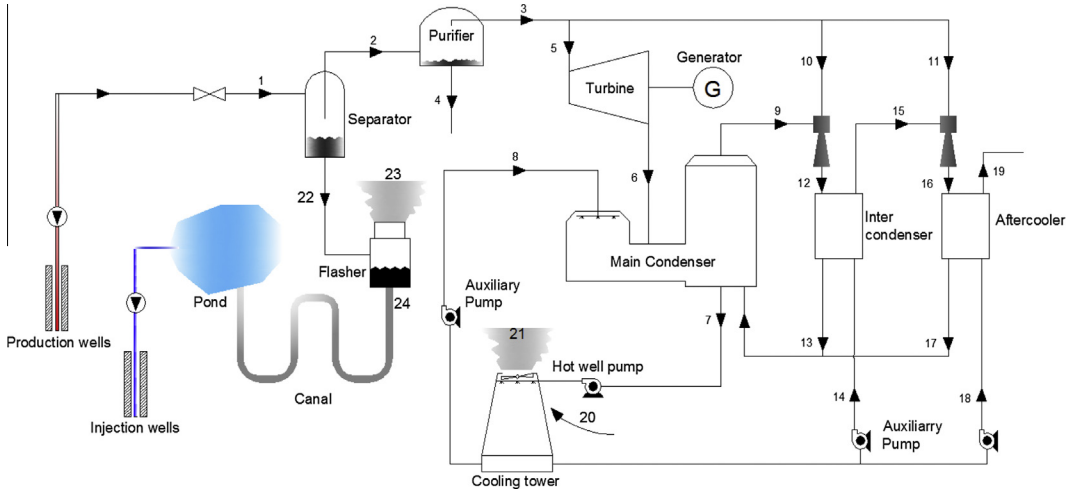

Fig. 2. Schematic diagram of single-flash geothermal power plant.

A hot well pump, which consumes 1.280 MW of electricity, works at the condenser to send the condensate water from the condenser into the cooling tower. The condenser is a direct contact-type, working with a cooling water–steam mixture. The cooling tower circulates the cooling water, indicated by numbers 8, 14 and 18, into the main condenser, the intercondenser and the aftercooler, using the auxiliary pump.

The non-condensable gas (NCG) is extracted from the system using a steam ejector, which is most commonly used in the gas removal systems of geothermal power plants [19]. Two ejectors are installed at this power plant: the intercondenser and the aftercooler. The first ejector removes the NCG from the main condenser, while another ejector removes the NCG from the intercondenser.

3. Analysis method

This research aims to analyze a single-flash system design to achieve optimum energy use employing an energy and exergy analysis based on the first and second laws of thermodynamics. The exergy equation can be expressed in Eq. (4) as follows [20]:

$$\dot{X}_i = \dot{m}_i[(h_i - h_0) - T_0(s_i - s_0)] \tag{4}$$

where $\dot{X}_i$ is exergy at stream i, $\dot{m}_i$ is mass flow rate at stream i, h_i is specific enthalpy at stream i, h_0 is specific enthalpy at environmental state, T_0 is temperature at environmental state, s_i is specific entropy at stream i, s_0 is specific entropy at environmental state.

The equation can be used to calculate the amount of exergy in any part of the power plant. From the calculated amounts of exergy, the exergy destruction can then be calculated. The results can be used to improve the thermal system to reach optimal conditions.

4. Second law efficiency

To evaluate the performance of the power plant relative to the exergy, a second law efficiency analysis can be used. Dipippo (2004) wrote that the second law efficiency can be defined as brute-force and functional approach. The brute-force approach is calculated by dividing the sum of all desired exergy outputs to necessary input as expressed in Eq. (5).

$$\eta_{II} = \frac{\sum \dot{X}_{out}}{\sum \dot{X}_{in}} \tag{5}$$

where $\sum \dot{X}_{out}$ is the total desired exergy output and $\sum \dot{X}_{in}$ is the total necessary exergy input. Each component of the power plant has several exergy inputs and outputs, and these components are summed, as shown in Eq. (5). For example, of these exergy inputs and outputs, in the separator, the exergy necessary input comes from the production well in the form of a steam–water two-phase mixture, while the desired exergy output accounts for the steam and the brine that flow out of the separator

The other definition of exergy efficiency based on a functional approach divides the desired exergy output into the exergy input that is needed in the process. The whole plant process uses this definition which uses turbine shaft-work as desired exergy output. This can be expressed mathematically as follows [20]:

$$\eta_{II} = \frac{\dot{W}_{net}}{\dot{X}_{in}}. \tag{6}$$

where $\dot{W}_{net}$ is the work produced by the plant and $\dot{X}_{in}$ is the total exergy that has entered the plant. The exergy that has entered the system can be calculated using information from the fluid properties at the production wellhead. The second law efficiency can also be calculated for each component in the system.

$$\eta_{II} = \frac{\sum \dot{X}_{out}}{\sum \dot{X}_{in}} \tag{7}$$

5. Results and discussion

Table 1 presents the important parameters of the states of the power plant: enthalpy, pressure, entropy, mass flow rate, energy, and exergy. The quality of the steam at state 1 is calculated to be 0.317. The reference conditions used for exergy analysis are state 0, with 18 °C and 0.78 bar for the atmospheric temperature and pressure, respectively. The cooling tower employs air in stream 20 to decrease its temperature. This table is used to create a Grassmann diagram of the overall exergy flow. The mass flow rate of discharged fluid from reservoir at point 1 is calculated based on the mass flow rate of the steam entering the turbine. This mass flow rate of steam is obtained from available plant data.

Table 2 summarizes the calculated exergy values and second law efficiency values at the various components of the plant. The exergy flow in such a system consists of the input and output exergies corresponding to the mass flow entering and leaving the system, respectively.

For the first component in the table, the separator has an exergy input from the steam–water mixture through the well of 59.52 MW. This exergy is calculated based on the mass flow rate entering the plant, the enthalpy and the entropy. These properties

Table 2
Calculated exergy values and second law efficiency at the components of the plant.

Component	Exergy input (MW)	Exergy output (MW)	Second law efficiency η_{II} (%)
Separator	59.52	51.48	86.50
Scrubber	37.96	37.82	99.63
Turbine-generator	35.05	21.73	61.99
Condenser	9.14	5.71	62.47
Intercondenser	1.39	0.46	32.81
Aftercooler	1.96	0.52	26.58
Cooling tower	5.62	3.00	53.41
Flasher	13.52	10.53	77.87
Overall plant	59.52	21.71	36.48

are determined by assuming the reservoir temperature value under liquid saturated conditions. The exergy outputs leaving the separator consist of the steam that is being transported to the turbine and the brine flowing to the reinjection wells. The second law efficiency of this component is 86.5%, as determined by dividing the output exergy by the input exergy. The process that occurs within the system is irreversible because of friction and heat transfer in several component parts of the equipment. The turbine-generator has a significant role in converting the thermal energy into electricity. The actual data of the power plant is used to calculate the exergy on this component.

The second law analysis calculation is performed by dividing the exergy output by the exergy input. The second law efficiency of the separator is estimated to be 86.50%. This second law efficiency is influenced by the enthalpy of the fluid from the reservoir and the ambient temperature in Dieng. Another second law efficiency value at a separator was calculated as 68% in the Olkaria power plant [21]. This low efficiency is because of the high enthalpy value of the fluid, reaching more than 2000 kJ/kg, and the high ambient temperature of 20 °C at that plant. For the plant overall, the second law efficiency is calculated to be 36.48%. This comes from the output power produced divided by the exergy input obtained from the geothermal fluid.

The amounts of the input and output exergies and the second law efficiencies for the plant components, such as the separator, scrubber, turbine-generator, condenser, intercondenser, the aftercooler, and the cooling tower are presented in Table 2. It is found that the highest second law efficiency occurs in the scrubber.

5.1. Thermodynamic processes

A temperature–entropy (T–s) diagram is shown in Fig. 3 that represents the thermodynamic process of the geothermal fluid in the Dieng geothermal power plant system. Initially, the geothermal fluid is discharged from the reservoir in the form of a single-phase liquid in saturated condition. The fluid then flows to the well head and flashes in the separator. The geothermal fluid produced from the reservoir through the well is initially in the single liquid-phase of compressed water in the reservoir. It is assumed that the geothermal fluid flows in an isenthalpic manner from the reservoir to the wellhead through the wellbore. During this process, the fluid starts flashing in the well, and both the temperature and the pressure decrease as the fluid reaches the wellhead in the two-phase condition.

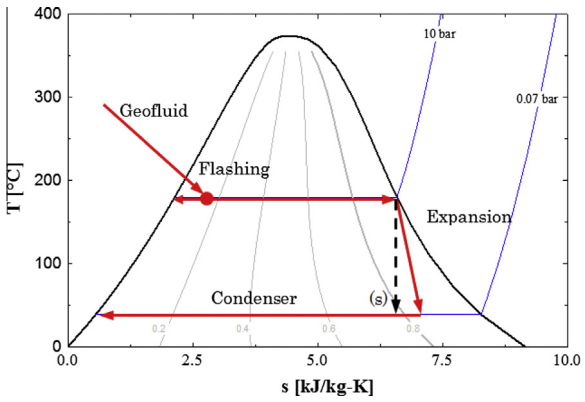

Fig. 3. Temperature–entropy (T–s) diagram.

At the separator, the steam and the brine are separated under isobaric conditions at a pressure of 10 bar. The separated steam flows into the turbine through the scrubber unit, and flows continuously to the turbine. The steam conditions at the turbine inlet, such as the temperature, pressure, and mass flow rate, are obtained from actual data from the plant. The temperature and pressure data of the turbine exhaust from the plant are also used. The dashed arrow in Fig. 3 indicates the isentropic expansion of the steam in the turbine. Because the turbine output and the steam properties in the turbine inlet are known, the isentropic efficiency can then be calculated to be 0.729.

The brine that is discharged from the separator first flows to the flasher, and then flows through the water canal inside the wellpad and out into the pond. The brine in the pond is pumped to the reinjection wells. The steam exhausted from the turbine then flows to the condenser for cooling and extraction of the non-condensable gases (NGG) by using the gas ejector.

5.2. Grassmann diagram

The Grassmann diagram in Fig. 4 describes the exergy flow entering and leaving the power plant and the losses. The total exergy input to the system is estimated to be 59.52 MW, which arrives from the reservoir in the form of a steam–water mixture, and produces a power output of 21.71 MW.

The exergy loss at the scrubber is not shown, because the amount of this loss is small in comparison with other losses. The condenser consists of three components: the intercondenser, main condenser, and aftercooler, which have exergy losses of 0.93 MW (1.57%), 3.43 MW (5.76%) and 1.44 MW (2.42%), respectively. This equipment consumes 9.75% of the total exergy. The separator loss is 8.04 MW (13.50%) and the turbine loss is 7.51 MW (12.62%). The loss from the flasher is quite high at 2.99 MW (5.03%). The exergy waste of the brine being sent back to the reservoir is significantly large at 10.70 MW. This constitutes 17.98% of the total input of exergy in this system. Also, the Dieng geothermal power plant uses a cold brine injection system, and this means that part of the exergy is lost to the environment as the brine vaporizes in the canal and the pond.

5.3. Optimization of single-flash system design

The power plant produces 21.71 MW of electricity with a separator pressure of 10 bar. To maximize the generated output power,

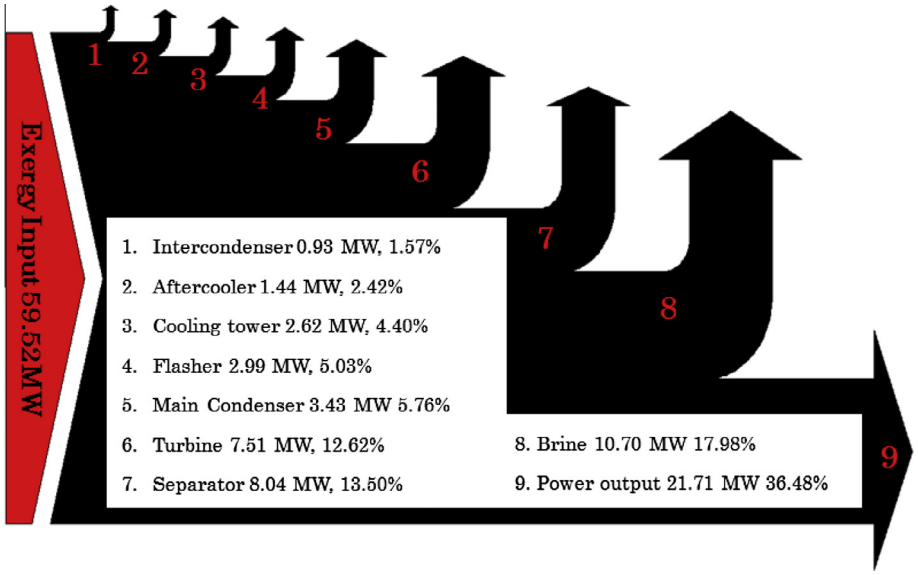

Fig. 4. Grassmann diagram for exergy flow and losses in power plant system.

the separator pressure is a candidate parameter for adjustment in sensitivity analyses. Thus, the relationship between the output power and the dryness fractions is calculated by varying the separator pressure. Because the separator pressure controls the steam mass flow rate at the separator that flows into the turbine, the output power can be increased.

The results of this analysis are shown in Fig. 5. It was found that a separator pressure of 9 bar produces the maximum electricity of 21.73 MW. Controlling this parameter with that pressure only produces 20 kW of additional electricity. The dryness fraction of the fluid produced increases with decreasing separator pressure, indicating that more steam can be delivered to the turbine. At 9 bar of separator pressure, the power plant has its highest power output and the dryness fraction is 32.39, which is an increase of only 2.24% from the initial condition.

Fig. 6 shows the steam and brine flow rates as a function of the separator pressure. The steam flow rate decreases as the separator pressure increases. This relationship occurs because of changes in the dryness fraction, as shown in Fig. 5. By lowering the separator pressure, the dryness fraction increases and this results in more steam being produced. We calculated that the steam mass flow rate under optimal conditions is 45.03 kg/s, while the brine mass flow rate is 79.27 kg/s.

We should note that if the separator pressure is changed, then the quality of the steam at the turbine outlet also changes. Fig. 7 shows the steam quality at the turbine outlet as a function of separator pressure. Increasing separator pressure leads to a decrease in the steam quality at the turbine outlet. In this optimization case, the separator pressure is lowered from 10 bar to 9 bar to produce more output power. Therefore, the steam quality increases slightly from 0.8642 to 0.8672, based on our calculations. There is also

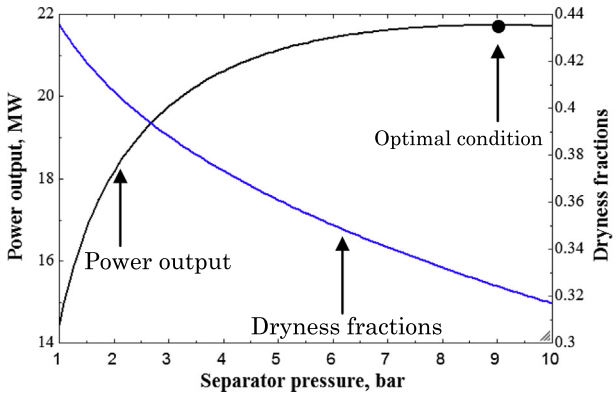

Fig. 5. Power output and dryness fractions as functions of separator pressure.

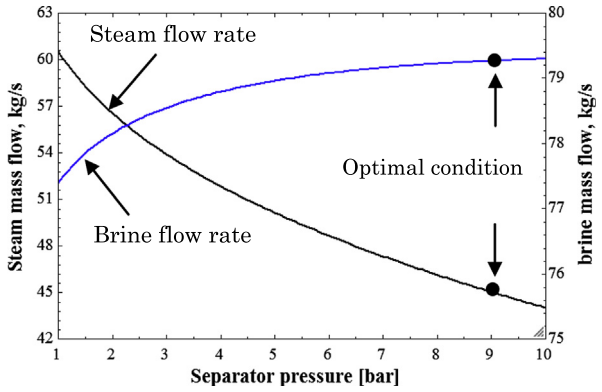

Fig. 6. Steam and brine mass flow rates as functions of separator pressure.

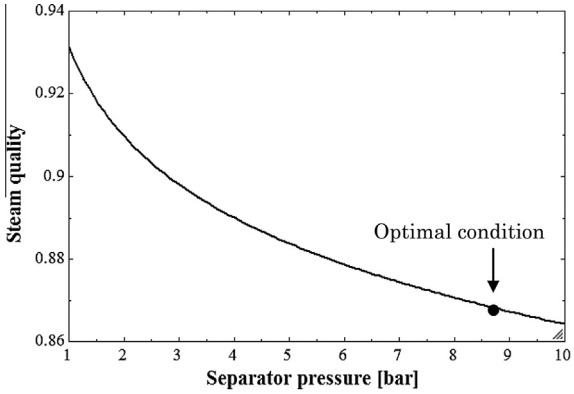

Fig. 7. Steam quality at the turbine outlet as a function of separator pressure.

other optimization of the plant using the double-flash system by utilizing 10.70 MW of waste brine that disposed to the environment.

6. Conclusions

Exergy analysis and sensitivity analysis for optimization of the Dieng geothermal power plant were performed by developing a mathematical model of the plant. Calculations were conducted by using EES software using methods based on the laws of thermodynamics.

The results showed that the total available exergy in the fluid produced from the production wells is calculated to be 59.52 MW. From this total, 21.71 MW is converted to electricity and 10.70 MW is lost in the brine canal and the pond before the brine is injected back to the reservoir.

The Grassmann diagram shows the exergy losses at each component in the power plant. Waste brine accounts for 17.98% of the total available exergy. The turbine and separator losses are 7.51 MW (12.94%) and 8.04 MW (13.50%), respectively, while the cooling tower has a 2.62 MW (4.40%) exergy loss. The total condenser losses, consisting of losses from three components (main condenser, intercondenser and aftercooler), are 9.75 MW (9.75%). The scrubber has the lowest exergy loss when compared with the other components at only 0.34 MW (0.24%).

The results of the optimization process show that the Dieng geothermal power plant operates under close to optimal conditions. This optimization process has provided a small improvement in the output power, which was 20 kW higher when we lowered the separator pressure to 9 bar. This optimization has also enhanced the steam quality at the turbine outlet. To utilize the 10.70 MW of waste brine that disposes to the environment, the double-flash system can be proposed to optimize the power output of the plant.

Acknowledgements

The authors would like to thank PT Geodipa Energy for their support in our research activities on the Dieng power plant and for the data provided. The authors would also like to thank the GCOE program at Kyushu University for their financial support.

References

[1] Aneke M, Agnew B, Underwood C. Performance analysis of the Chena binary geothermal power plant. Appl Therm Eng 2011;31:1825–32.
[2] Ármannsson H, Fridriksson T, Kristjánsson BR. CO_2 emissions from geothermal power plants and natural geothermal activity in Iceland. Geothermics 2005;34:286–96.
[3] DiPippo R. Geothermal power plants, principles, applications, case studies and environmental impact. 2nd ed. Elsevier; 2005.
[4] Zhoua C, Doroodchib E, Moghtaderia B. An in-depth assessment of hybrid solar–geothermal power generation. Energy Convers Manage 2013;74:88–101.
[5] Bertani R. Geothermal power generation in the world 2005–2010 update report. Geothermics 2012;41:1–29.
[6] Agugliaroa FM, Alcaydea A, Montoyaa FG, Sierraa AZ, Gilb C. Scientific production of renewable energies worldwide: an overview. Renew Sust Energy Rev 2013;18:134–43.
[7] Darma S, Harsoprayitno S, Setiawan B, Hadyanto, Sukhyar R, Soedibjo AW, Ganefianto N, Stimac J. Geothermal energy update: geothermal energy development and utilization in Indonesia. World geothermal congress 2010. Bali, Indonesia.
[8] Dincer I, Rosen MA. Exergy, energy, environment and sustainable development. Elsevier; 2007. p. 454. ISBN: 978-0-08-044529-8.
[9] Dağdaş A, Öztürk R, Bekdemir S. Thermodynamic evaluation of Denizli Kızıldere geothermal power plant and its performance improvement. Energy Convers Manage 2005;46:245–56.
[10] Ozgener L, Hepbasli A, Dincer I. Energy and exergy analysis of Salihli geothermal district heating system in Manisa, Turkey. Int J Energy Res 2005;29:393–408.
[11] Balli O, Aras H, Hepbasli A. Exergetic performance evaluation of a combined heat and power (CHP) system in Turkey. Int J Energy Res 2007;31:849–66.
[12] Rosen M, Tang R, Dincer I. Effect of stratification on energy and exergy capacities in thermal storage systems. Int J Energy Res 2004;28:177–93.
[13] Cengel YA. Green Thermodynamics. Int J Energy Res 2007;31:1088–104.
[14] Rosen MA. Second-law analysis: approaches and implications. Int J Energy Res 1999;23:415–29.
[15] Suberi I. Integrated control of late blight (Phytophtora infestans) in potatoes in the Dieng plateau and Banjarnegara [in Indonesia]. Report.
[16] Junaldi, Indriawati K. Prediction of power output geothermal power plant based on weighted moving average method in Geodipa energy company, Dieng unit. Jurnal Teknik Pomits 2012;1:1–6 [in Indonesia].
[17] Hochstein MP, Sudarman S. History of geothermal exploration in Indonesia from 1970 to 2000. Geothermics 2000;37:220–66.
[18] Prasetio R, Abidin Z, Yulizar, Y. Isotope and gas geochemistry of Dieng geothermal field, Indonesia, In: Proceedings, world geothermal congress, Bali, Indonesia. 2010; 25–29 April.
[19] Yildirim NO, Gokcen G. Thermodynamic assessment of gas removal systems for single-flash geothermal power plants. Appl Thermal Eng 2009;29:3246–53.
[20] Cengel YA, Boles MA. Thermodynamics: an engineering approach. McGraw-Hill; 1989.
[21] Clety BK. Exergy analysis of Olkaria power plant, Kenya, Geothermal training program. Report 2005.